METROLOGY AND MEASUREMENT SYSTEMS
VOL. XV, NUMBER 4 (2008)

WOJCIECH FRĄCZEK, JANUSZ MROCZKA

Wroclaw University of Technology
Chair of Electronic and Photonic Metrology
Wroclaw, Poland
e-mail: wojciech.fraczek@pwr.wroc.pl

OPTICAL VORTICES AS PHASE MARKERS TO WAVE-FRONT DEFORMATION MEASUREMENT

In this paper a new method to the test deformation of the wave-front of the plane wave is presented. In the method Optical Vortex Interferometry is applied. In the OVI a regular lattice of optical vortices is generated by the interference of three plane waves. The wave-front of one wave is deformed after crossing the measured object. The deformation of the wave-front is measurable because the deformation of vortex lattice structure arises from the wave-front deformation. The record of the positions of the vortex points before and after the object insertion in the optical arrangement is essential. The analysis of the change of vortex points positions, as shown in this paper gives highly precise information about the real deformation of the wave-front caused by the object insertion.

Keywords: optical vortices, interferometry, wave-front.

1. INTRODUCTION

Optical Vortices (OV's) are isolated singularities in the phase distribution of the optical wave-field [1]. They have some special properties, which have been studied in the last decade [2]. The OV's are the subject of many scientific tasks. One of them is an Optical Vortex Interferometer (OVI) [3]. The OVI is a kind of a multiple beam interferometer which uses interference of three beams (in other applications which are not described in this paper more beams may be used [4]). In the OVI a regular lattice of OV's is generated by the interference of the three plane beams. The OVI may be used in a new method of wave-front deformation test. In this method the dislocation of the OV's is used to calculate wave-front deformation caused by the parallel glass plate insertion in the path of one of the beams. Therefore the record of the positions of the vortex points before and after parallel glass plate insertion in the optical arrangement is essential. One wave in the OVI is deformed after crossing the measured parallel glass

[1] Received: October 16, 2008. Revised: November 24, 2008.

plate. The deformation of the wave-front is measurable because the deformation of the vortex net structure arises from the wave-front deformation. The analysis shown in this paper of the dislocations of the vortex points shown in this paper gives highly precise information about the real shape of the parallel glass plate. The precision depends on the OV's localisation accuracy [5]. Additionally, the described method provides solution to the problem how to determine where the surface is convex and where it is concave. The OV may have two opposite topological charges corresponding to the orientation of the wave-front screw. The sign of the topological charge of the optical vortex can be determined [6]. The knowledge about the topological charge of the vortices in the net resolves where the surface is convex or concave.

The interferograms described in this paper can be obtained in the optical arrangement shown in Fig. 1. The main part of the OVI is the set of six beamsplitters. The beamsplitters are adjusted so as to obtain a regular hexagonal net of OV's by the interference of the three plane beams (A,B and C) without the parallel glass plate (GP). We use a He-Ne laser (632,8nm) and 12bit CCD camera 1344×1024 pix. with the cell size 6,45×6,45 μm. All simulations in this paper correspond to this equipment. The interferogram obtained by the three plane waves interference, with the hexagonal regular net of optical vortices, is shown in the Fig. 2 (Fig. 2a). Additionally in (Fig. 2b) coordinates of vortex points (VP's) are marked. Coordinates of the VP's can be obtained with the use of one of localization methods of the vortex ponts [5]. The localization methods are described in other publications. The theoretical analysis chosen to test the method are described in the next section of the paper. The presented method can be applied in another optical vortex interferometer [7] as well.

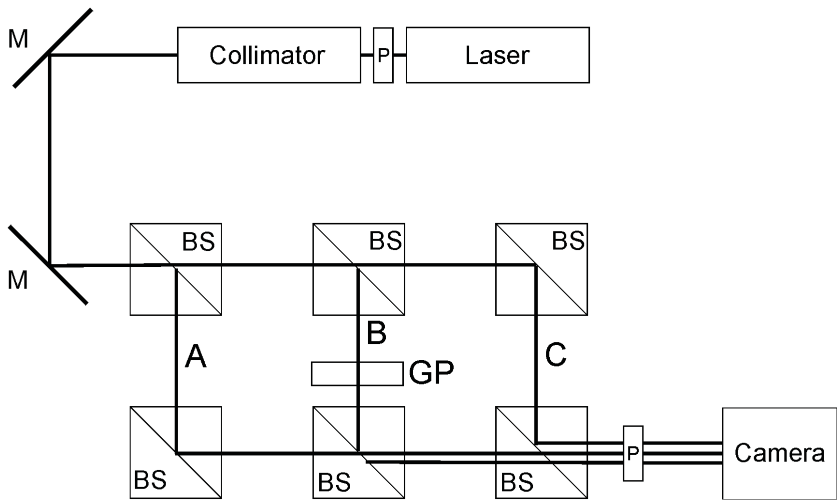

Fig. 1. Block diagram of the OVI with tested Glass Plate (GP).

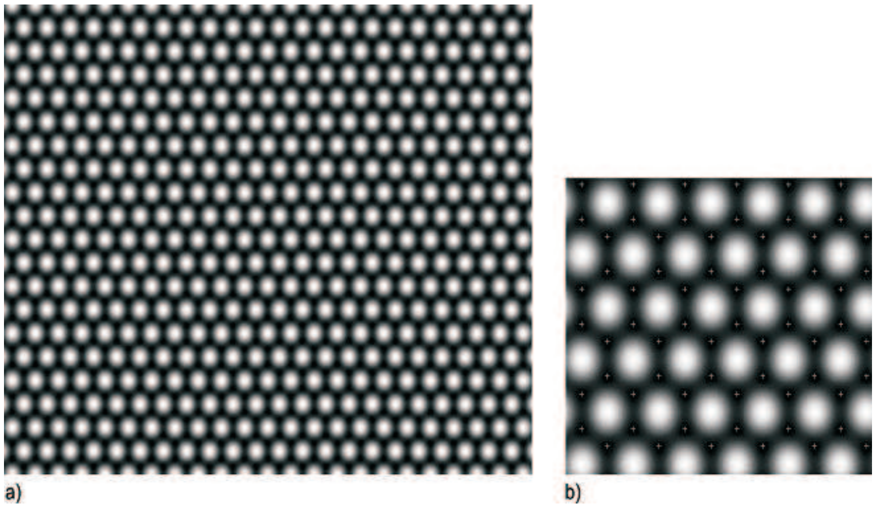

Fig. 2. Interferogram obtained by the three plane waves (A,B and C) interference a) – interferogram b) – part of interferogram with VP's marked.

2. THEORETICAL ANALYSIS

2.1. Data

First we prepare three sets of data. We decide to test the method in three cases: FIRST: ideal situation with three beams without wave-front deformation, SECOND: situation with a small wave-front deformation.

$$\varphi = 0.05 \cdot \sin\left(4 \cdot \pi \cdot \frac{x}{X}\right) + 0.05 \cdot \sin\left(4 \cdot \pi \cdot \frac{y}{Y}\right), \tag{1}$$

where: φ – phase, [X,Y] – CCD size, [x,y] coordinate.

THIRD: situation with a big wave-front deformation

$$\varphi = \sin\left(4 \cdot \pi \cdot \frac{x}{X}\right) + \sin\left(4 \cdot \pi \cdot \frac{y}{Y}\right) + \sin\left(4 \cdot \pi \cdot \frac{\sqrt{x^2 + y^2}}{\sqrt{X^2 + Y^2}}\right). \tag{2}$$

In contrast to the FIRST and SECOND situations, the deformation in the THIRD situation can be seen with the naked eye in the interferogram.

When we measure a real object we should record an interferogram like the one shown in Fig. 2. Moreover we may record three other interferograms with fringe patterns obtained by the two – wave interference (AB, BC and CA). To test the method we generated interference patterns numerically. Two simulated waves were plane (A and C). The third wave (B) was generated with non – planar wave-front. The generated

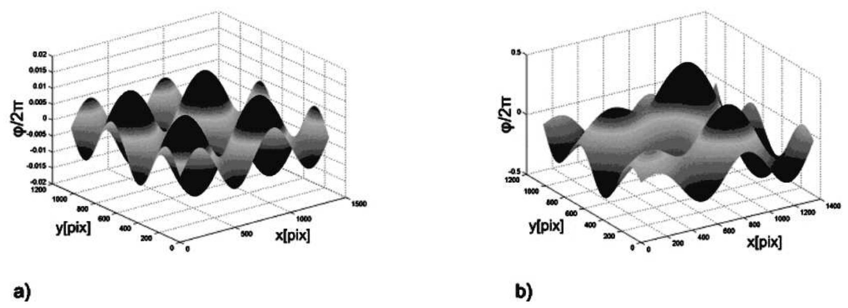

Fig. 3. Wavefront deformations generated in a) – SECOND situation, b) – THIRD situation.

deformation is shown and described above. The generated interferograms are treated as measured data without the knowledge about the wavefront shape during data analysis. The end result of the wave-front reconstruction is compared with the theoretical equations.

2.2. Data analysis

At the beginning of the data analysis in the presented method it is necessary to localize the VP's and to determine the sign of topological charge. Methods of the VP's localization are described in other publications and any of these may be used. A similar situation is with the methods of determination of the topological charge sign.

Next the OV's must be split into two groups according to on the topological charge. At this stage the groups must be analyzed separately because of the phase difference between vortex points of vortices with positive and negative signs.

If the amplitude of each wave is constant in the analyzed area then the relative phases between two waves in VP's from one group are the same (in 2π range). Next we obtain two values of the relative phase between the two chosen waves (for example A and B), $\varphi+$ and $\varphi-$ appropriately to the sign of the topological charge. In this case the amplitude of each wave is the same, the two values equal $2\pi/3$ and $4\pi/3$, respectively.

Coordinates of the VP's from two groups are presented in Fig. 4. Vortex points from one group are marked by 'x' and those from the second group are marked by 'o'. In Fig. 4, each line contains the coordinates of the VP's where the relative phases between two waves are the same. All neighboring lines of the same type (e.g. dashed) contain VP's where the relative phase is changed by 2π. In Fig. 4 a) the lines that are used to analyze relative phase between waves C and A are shown. In Fig. 4 b) there lines which are used to analyze the relative phase between waves A and B are shown. The lines in the Fig. 4 a) are straight because the wave-fronts A and B are plane. Because the wavefront of wave B is not plane, the lines in Fig. 4 b) are not straight. In the next step the wavefront distortions are calculated.

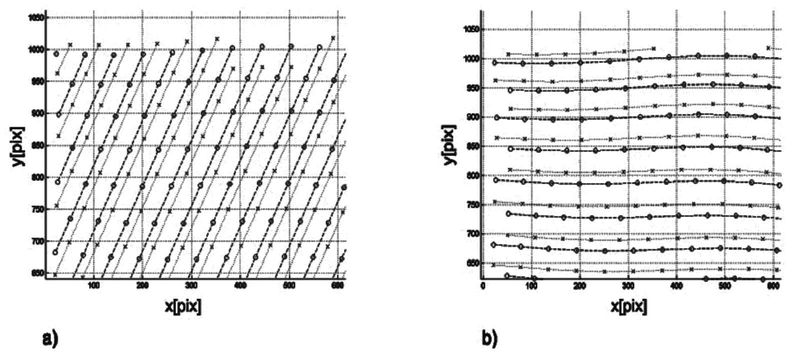

Fig. 4. VP's coordinates and lines which are used to analyze the relative phase between waves a) – C and A, b) – A and B.

At this stage it is important which group of the vortices has a positive sign and which has a negative one. In the analyzed case the vortex marked by 'x' has a positive sign of topological charge and the vortex marked by 'o' an opposite sign. If the lines from Figure 4 b) are numbered from bottom to the top, the relative phase decreases for every following line of the type by 2π. The result of this operation is shown in Fig. 5. If the surface is approximated by the plane and the differences between the plane and the points from the non-plane surface are calculated then the shape of the wave-front is obtained.

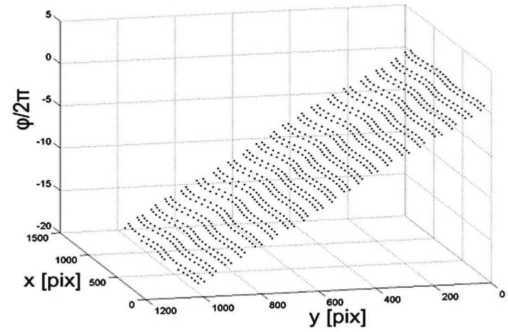

Fig. 5. Relative phase between waves A and B in vortex points.

2.3. Results

After applying the data analysis described in point 2.2 for data described in point 2.1 we obtained the results shown below.

In Fig. 6 the obtained wavefront shapes after calculations for the FIRST case are presented. The wave-front should be plane but errors in the VP's localization and numerical interferograms analysis lead to differences between the theoretically calculated and the reconstructed by about $3*10^{-3}\lambda$.

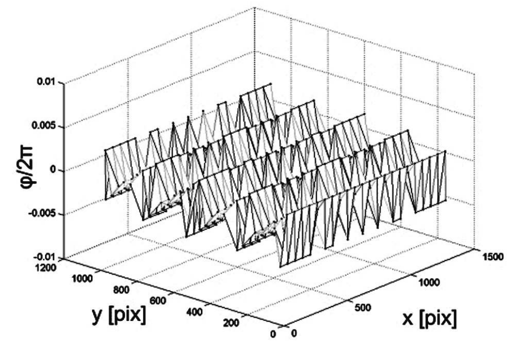

Fig. 6. Reconstructed wavefront shape of the wave B in the FIRST case (without the wave-front distortion).

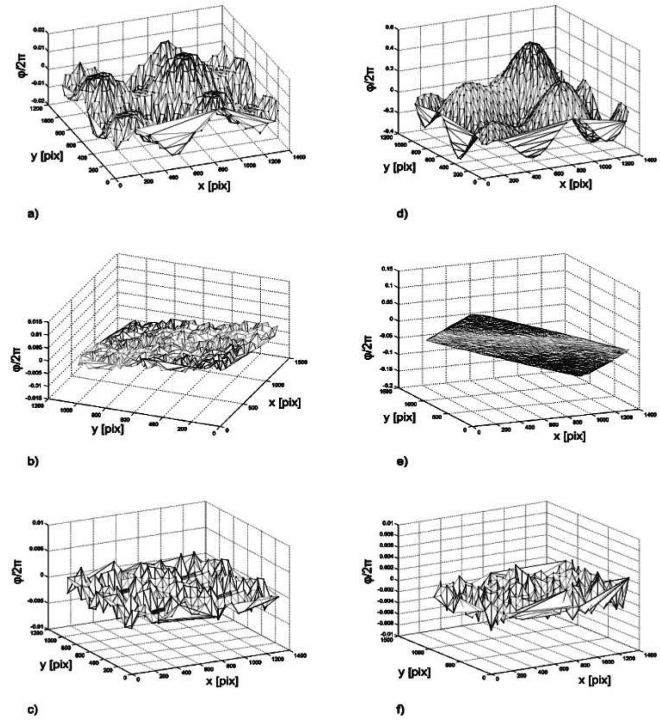

Fig. 7. Results of reconstructions. a), b), c) – the SECOND case, d), e), f) – the THIRD case, a), d) – the wave-front of the wave B, b), e) – errors of the reconstructions, c), f) – the wave-front of the wave C.

Because the wave B (with or without the wavefront deformation) interferes with two plane waves A, the wavefront of the wave B is obtained from the relative phase between the waves B and A. The vortex points are used as markers because the relative phase in these points is known. In Fig. 7 results of the reconstructions for two cases (the SECOND and the THIRD) are shown. For both cases:
a) and d) the results of the wave B wave-fronts reconstructions,
b) and e) the errors of the wave B wave-fronts reconstructions,
c) and f) the results of the wave C wave-fronts reconstructions, are presented.

The wave-front of the wave C is plane so Fig. 7 c) and d) should a present the plane surface, unlike in the FIRST case.

The errors of the reconstruction were calculated as a difference between the reconstructed wavefront deformation and deformation from point 2.1 adequately to the case FIRST, SECOND or THIRD.

3. CONCLUSION

The method presented in this paper may be applied to the test a deformation of a wave-front caused by optical equipment. Theoretically, the precision of the method may be about $3*10^{-3}\lambda$. The precision strongly depends on the accuracy of the localization method. The method can be applied to the test reflective surface in a similar optical arrangement. Unfortunately the presented data analysis cannot be the final version because of the reconstruction error. The reconstruction error is sloped almost as a plane surface and may be eliminated. This reconstruction error arises from the reference plane obtained from the relative phase between waves A and B (Fig. 5). After correcting the slope of the reference plane the reconstruction error may be decreased to $3*10^{-3}\lambda$.

ACKNOWLEDGMENTS

The article is published with the support of the Foundation for Polish Science.

REFERENCES

1. Vasnetsov M., Staliunas K.: *Optical Vortices* Nova Science Publishers 1999.
2. Desyatnikov A.S., Torner L., Kivshar Yu. S.: "Optical Vortices and Vortex Solitons". *Progress in Optics*, E. Wolf (Ed.), 2005, p.47.
3. Masajada J., Dubik B.: "Optical vortex generation by tree plane wave interference". *Optic Communication 198*, 2001, pp. 21–27.
4. Masajada J., Popiołek-Masajada A., Leniec M.: "Creation of vortex lattices by a wavefront division". *Opt. Express*, vol.15, no. 8, 2007, p.5196.

5. Masajada J., Popiołek-Masajada A., Frączek E., Frączek W.: ”Vortex points localization problem in optical vortices interferometry”, *Optic Communication 234*, 2004, pp. 23–28.
6. Frączek E., Frączek W., Mroczka J.: ”The experimental method for tophological charge determination of optical vortices in a regular net”. *Optical Engineering 44 (2)*, 25601, 2005.
7. Kurzynowski P., Wożniak W.A., Frączek E.: ”Optical vortices generation using the Wollaston prism”, *App. Opt.*, vol.45, no. 30 (2006), pp. 7898–7903.